Limnol. Oceanogr., 56(6), 2011, 2040–2050

doi:10.4319/lo.2011.56.6.2040

Distinguishing between the effects of ocean acidification and ocean carbonation in the coccolithophore *Emiliania huxleyi*

Lennart Thomas Bach,* Ulf Riebesell, and Kai Georg Schulz

Leibniz Institute of Marine Sciences (IFM-GEOMAR), Kiel, Germany

Abstract

The coccolithophore *Emiliania huxleyi* was cultured under a broad range of carbonate chemistry conditions to distinguish the effects of individual carbonate system parameters on growth, primary production, and calcification. In the first experiment, alkalinity was kept constant and the fugacity of CO_2 (fCO_2) varied from 2 to 600 Pa (1 Pa $\approx$ 10 μatm). In the second experiment, pH was kept constant (pH_{free} = 8) with fCO_2 varying from 4 to 370 Pa. Results of the constant-alkalinity approach revealed physiological optima for growth, calcification, and organic carbon production at fCO_2 values of $\sim$ 20 Pa, $\sim$ 40 Pa, and $\sim$ 80 Pa, respectively. Comparing this with the constant-pH approach showed that growth and organic carbon production increased similarly from low to intermediate CO_2 levels but started to diverge towards higher CO_2 levels. In the high CO_2 range, growth rates and organic carbon production decreased steadily with declining pH at constant alkalinity while remaining consistently higher at constant pH. This suggests that growth and organic carbon production rates are directly related to CO_2 at low (sub-saturating) concentrations, whereas towards higher CO_2 levels they are adversely affected by the associated decrease in pH. A pH dependence at high fCO_2 is also indicated for calcification rates, while the key carbonate system parameter determining calcification at low fCO_2 remains unclear. These results imply that key metabolic processes in coccolithophores have their optima at different carbonate chemistry conditions and are influenced by different parameters of the carbonate system at both sides of the optimum.

With the beginning of the industrial revolution in the late 18th century, humankind started to considerably increase the atmospheric carbon dioxide (CO_2) concentration mainly due to burning of fossil fuels and deforestation of vast regions. This increase would have been even more pronounced if the ocean had not absorbed $\sim$ 30% of anthropogenic CO_2 (Sabine et al. 2004). The flip side of the invasion of anthropogenic CO_2 into the ocean (i.e., ocean carbonation) is a decreasing seawater pH—a problem that is referred to as ocean acidification. The surface seawater pH has already decreased by 0.1 pH units since preindustrial times and might further decrease about 0.3–0.4 pH units by the year 2100 (Wolf-Gladrow et al. 1999; Caldeira and Wickett 2005). Ocean acidification and ocean carbonation lead to changes in the concentrations of CO_2, HCO_3^-, CO_3^{2-}, and H^+ in seawater. The effect of these projected changes on different cellular processes such as photosynthesis and calcification is not yet fully understood.

Phytoplankton produces organic carbon via photosynthesis, thereby forming the basis of the marine food web. Coccolithophores constitute an important group of phytoplankton. Their characteristic feature is the production of small scales (coccoliths) made of calcium carbonate ($CaCO_3$) which cover the cell. The response of coccolithophores to projected changes in carbonate chemistry has been studied extensively in the past (reviewed in Riebesell and Tortell in press). Most of these studies examined the response of coccolithophores to projected future ocean CO_2 scenarios (IPCC 2001) and found profound changes in growth rates, photosynthesis, and carbon fixation in response to increasing CO_2 levels. The study presented here focuses on the physiology of the coccolithophore *Emiliania huxleyi* (strain B92/11). The primary motivation was to determine optimum carbonate chemistry conditions for growth, primary production, and calcification rates of *E. huxleyi* and to elucidate which parameters of the carbonate system were responsible for the observed sensitivities.

Methods

Experimental setup—Two experiments are presented in this study, which are generally similar in design and growth conditions. Differences between the experiments are exclusively reflected in the carbonate system manipulation (*see* below).

Monospecific cell cultures of *Emiliania huxleyi* B92/11 (Plymouth Marine Laboratory) were grown in dilute batch cultures where *E. huxleyi* was harvested at low biomass (final cell numbers not exceeding 73,000 cells mL^{-1}) so that there was no significant change in the chemical or physical conditions of the culture medium (LaRoche et al. 2010). Cells grew at 15°C in artificial seawater at a photon flux density of 150 μmol m^{-2} s^{-1} and a 16 : 8 h light : dark cycle. Artificial seawater with a salinity of 35 was prepared as described in Kester et al. (1967) without the addition of $NaHCO_3$. The dissolved inorganic carbon (DIC)– and total alkalinity (TA)–free artificial seawater was enriched with $NaNO_3$ (nitrate) and Na_2HPO_4 (phosphate) to concentrations of $\sim$ 64 μmol kg^{-1} and $\sim$ 4 μmol kg^{-1}, respectively, and with trace metals and vitamins according to f/8 medium (Guillard and Ryther 1962). Concentrations of nitrate and phosphate were determined according to Hansen and Koroleff (1999) at the beginning and the end

* Corresponding author: lbach@ifm-geomar.de

of the experiments and indicated replete (non-limiting) concentrations for both nutrients throughout the experiments. The artificial seawater was further enriched with 10 nmol kg^{-1} of SeO_2 (Danbara and Shiraiwa 1999) and 2 mL kg^{-1} of natural North Sea water to provide possible other essential micronutrients that are not included in the recipe of Guillard and Ryther (1962). The medium was sterile filtered (0.2 μm) into sterile 2.5-liter polycarbonate bottles where the carbonate chemistry was adjusted (*see* below). After taking samples for TA or pH and DIC, the medium was gently transferred into sterile 2-liter polycarbonate bottles. Headspace in the experimental bottles was minimized to ~ 5 mL. Bottles were acclimated to the incubation temperature prior to inoculation from the precultures to avoid a potential thermal shock. Cells were acclimated to the growth and carbonate chemistry conditions of the main experiment for at least nine generations.

Carbonate chemistry manipulation—In the first experiment, TA was kept constant whereas fCO_2 was varied from 2 to 600 Pa (1 Pa ≈ 10 μatm). This experiment simulates ocean acidification and carbonation where both pH and CO_2 change ($_{variable}$pH). In the second experiment, pH was kept constant and fCO_2 was varied from 4 to 370 Pa. This experiment simulates ocean carbonation alone ($_{constant}$pH). At $_{variable}$pH, DIC levels were adjusted by adding calculated amounts of Na_2CO_3. TA was adjusted through calculated amounts of hydrochloric acid (3.571 molar, certified by Merck) to reach a constant value of ~ 2325 μmol kg^{-1} (± 22 μmol kg^{-1}) in all treatments (Gattuso et al. 2010). Carbonate chemistry of $_{constant}$pH was adjusted by adding 2 mmol kg^{-1} of 2-[-4-(2-hydroxyethyl)-1-piperazinyl]-ethanesulfonic acid (HEPES; pH_f [pH on free scale] ~ 8.0) and calculated amounts of $NaHCO_3$. The small change in pH by $NaHCO_3$ addition was compensated by additions of NaOH, resulting in a constant pH_f of ~ 8 (± 0.01) in all treatments.

Carbonate chemistry sampling and measurements—Samples for TA measurements were filtered (~ 0.7 μm), poisoned with a saturated $HgCl_2$ solution (0.5‰ final concentration), and stored at 4°C. TA was measured in duplicate, applying a two-stage potentiometric open cell titration (Dickson et al. 2003), and corrected with certified reference material (A. Dickson, La Jolla, California). DIC samples were sterile filtered (0.2 μm) by gentle pressure and stored bubble free in 4-mL borosilicate bottles at 4°C until photometrical measurement (Stoll et al. 2001).

Samples for pH were measured potentiometrically at 15°C with separate glass and reference electrodes (Metrohm), which were calibrated with certified reference material (A. Dickson, La Jolla, California). pH_f of the reference material was calculated from known TA and DIC, applying the constants of Roy et al. (1993). Measured electromotive force (E) of the samples and standards were used to calculate the pH_f of the sample, applying Eq. 1:

$$pH_f = pH_{f\_reference} + \frac{E_s - E_x}{R \times T \times \frac{\ln 10}{F}} \quad (1)$$

where $pH_{f\_reference}$ is the calculated pH_f of the certified reference material, E_s and E_x are the measured electromotive forces in volts of the reference material and the sample respectively, T is the temperature of the sample in kelvin, R is the universal gas constant, and F is the Faraday constant. This method of measuring pH is comparable to the potentiometric method described in Dickson et al. (2007) with the difference that instead of self-made buffers in synthetic seawater, reference material certified for DIC and TA is used. This was possible in our case because the salinity in the experiments (i.e., 35) is close to the salinity of the certified reference material (i.e., 33.3).

For DIC measurements, the DIC range in $_{constant}$pH, extending from ~ 180 to ~ 14,000 μmol kg^{-1} was far too large to be measured with recommended methods. Therefore, culture medium was mixed with artificial seawater of known DIC concentration immediately after culture bottles were opened for sampling. The ratio of the mixing solvent to the original DIC sample was determined by first weighing the mixing solvent alone and in a second step the mixing solvent plus the original DIC sample on a high-accuracy balance with a precision of ± 0.01 mg (Sartorius). The mixture was carefully rotated in a 50-mL tube with ~ 1-mL headspace. The ratio of sample to mixing solvent was adjusted to result in a final DIC concentration of 1800–2200 μmol kg^{-1}. From that point on, DIC samples were sterile filtered (0.2 μm) by gentle pressure and stored bubble free in 4-mL borosilicate bottles at 4°C until photometrical measurement (Stoll et al. 2001).

DIC estimations—Unfortunately, we lost all DIC measurements of $_{variable}$pH and the DIC measurements from the beginning of $_{constant}$pH due to storage problems. To obtain DIC concentrations from the beginning of $_{constant}$pH, we added the total particulate carbon buildup which was produced during the experiment to the final DIC concentrations. Initial DIC concentrations from $_{variable}$pH were calculated by taking advantage of the following conditions. The artificial seawater, which was used in $_{variable}$pH, was initially free of TA and DIC. Hence, TA and DIC were exclusively added as Suprapur® Na_2CO_3 (Merck). This means that the addition of 1 mole of Na_2CO_3 increased DIC by 1 mole and TA by 2 moles. Excess TA was removed in the following step by adding calculated amounts of certified HCl (3.571 mol L^{-1}, Merck) with no effect on DIC. Initial DIC concentration can then be calculated as:

$$DIC = \frac{TA_{measured} + (Volume_{acid} \times 3.571)}{2} \quad (2)$$

where $TA_{measured}$ is the measured TA in μmol kg^{-1} at the beginning of the experiment, $Volume_{acid}$ is the volume of acid that was added in μL kg^{-1}, and 3.571 is the molarity of the acid (certified by Merck) in μmol μL^{-1}. DIC concentrations at the end of $_{variable}$pH were calculated by subtracting the measured total particulate carbon buildup from the initial DIC concentrations.

Quality assessment of DIC estimations—There are potential sources of uncertainty on the DIC estimation

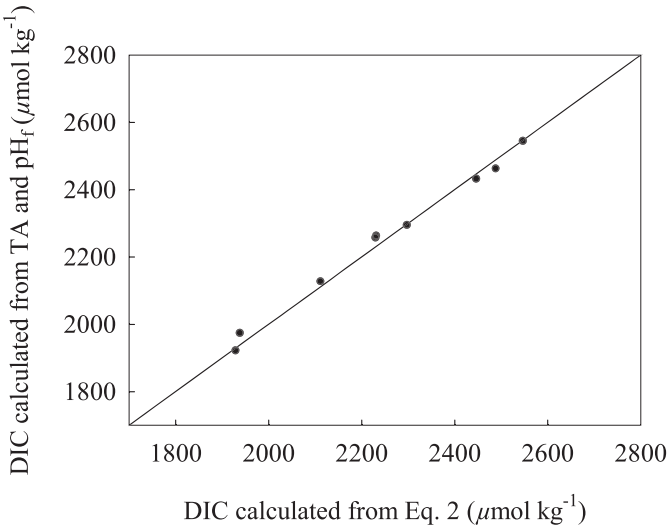

Fig. 1. DIC concentration calculated from TA and pH_f applying stoichiometric equilibrium constants by Roy et al. (1993) in relation to DIC concentration calculated from Eq. 2. The solid line denotes equal concentrations. The maximum offset between the two methods was 30 μmol kg^{-1}.

given above. The calculation of initial or final DIC values from total particulate carbon production does not account for buildup of dissolved organic carbon in the course of the experiments. To estimate whether this might have caused large deviations in DIC estimations, nine cultures of *E. huxleyi* were grown at different CO_2 levels at the same culture conditions as in the experiments presented in this study. We found that DIC drawdown is not systematically higher or lower than total particulate carbon buildup. The maximum difference between both measurements was 14 μmol kg^{-1}. Another source of uncertainty arises from the DIC estimation from total alkalinity measurements and acid addition given in Eq. 2. The quality of this procedure was tested by comparing DIC values calculated from measured TA and pH to those calculated from Eq. 2. We found a maximum difference of 30 μmol kg^{-1} between both DIC values (Fig. 1). In summary, there are uncertainties of 40–50 μmol kg^{-1} in the applied DIC estimations. These uncertainties are small compared to the large DIC range of $\sim$ 1200 μmol kg^{-1} in $_{variable}$pH and $\sim$ 13,800 μmol kg^{-1} in $_{constant}$pH and should therefore not affect the overall conclusions drawn in this study.

Carbonate chemistry calculations—Carbonate system parameters used to calculate carbonate chemistry in $_{variable}$pH were TA and the estimated DIC (*see* above). Carbonate system parameters used to calculate carbonate chemistry in $_{constant}$pH were measured pH_f and DIC where DIC was directly measured at the end of the experiment while it was estimated at the beginning of the experiment (*see* above).

The other carbonate system parameters and fCO_2 were calculated from temperature, salinity, measured inorganic phosphate concentrations, and the respective carbonate system parameters, using equilibrium constants of Roy et al. (1993) and the program CO2Sys (Lewis and Wallace 1998) (Fig. 2). Biological response data are plotted against the means of the initial and final values of the carbonate chemistry. Horizontal bars in Figs. 3, 4 denote the change in fCO_2 over the course of the experiment.

Sampling and processing of organic matter, inorganic matter, cell size, and cell numbers—Sampling started 2 h after the beginning of the light period and lasted no longer

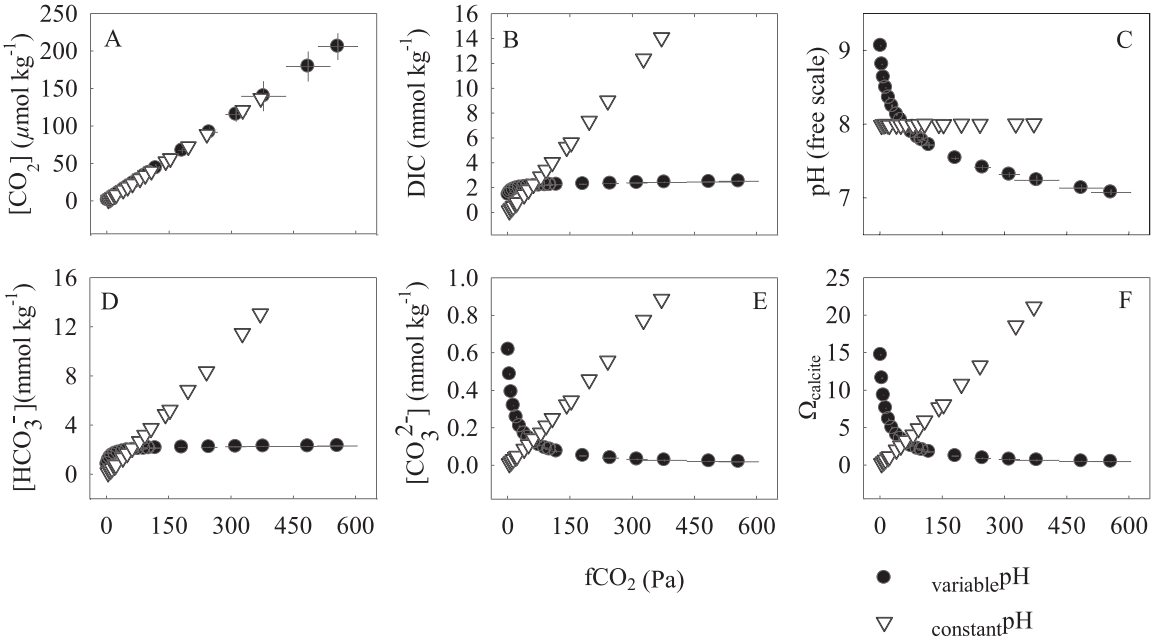

Fig. 2. Carbonate system parameters in $_{variable}$pH and $_{constant}$pH in relation to fCO_2. (A) [CO_2], (B) DIC, (C) pH, (D) [HCO_3^-], (E) [CO_3^{2-}], and (F) $\Omega_{calcite}$. Horizontal and vertical bars denote the change in the carbonate chemistry parameter over the course of the experiment. The response data are plotted against the means of the initial and final values of the carbonate chemistry.

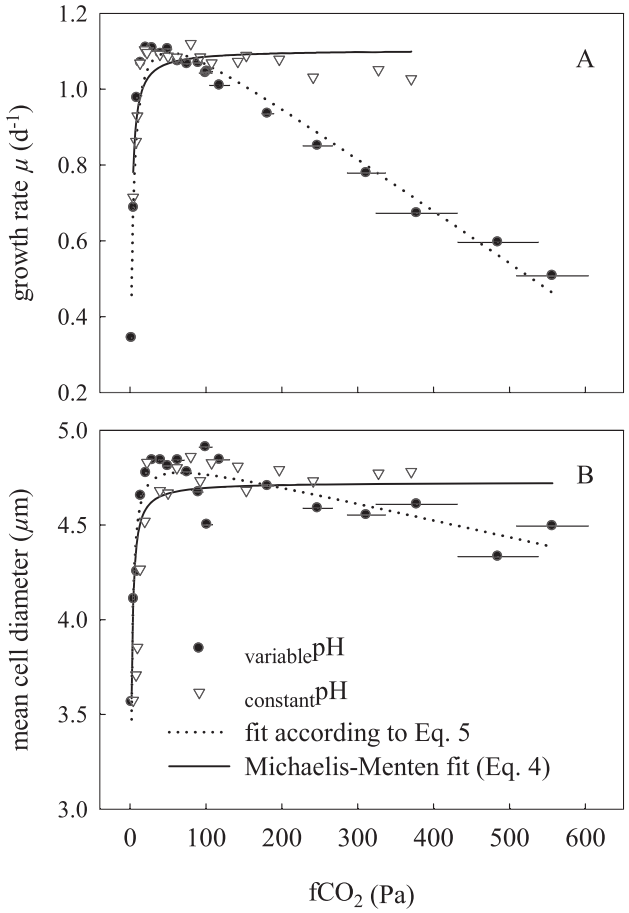

Fig. 3. Growth rates and mean cell diameter in $_{variable}$pH and $_{constant}$pH in relation to fCO_2. (A) Growth rates (dotted line $R^2 = 0.95$, $p < 0.0001$; solid line $R^2 = 0.74$, $p < 0.0001$). (B) Mean cell diameter (dotted line $R^2 = 0.86$, $p < 0.0001$; solid line $R^2 = 0.89$, $p < 0.0001$). Horizontal bars denote the change in fCO_2 over the course of the experiment. The biological response data are plotted against the means of the initial and final fCO_2 values.

than 2 h. Duplicate samples for total particulate carbon (TPC), particulate organic carbon (POC), and single samples for chlorophyll *a* (Chl *a*) were gently filtered (20 kPa) onto precombusted (5 h, 500°C) GF/F filters and stored in the dark at −20°C until measurements. Samples for TPC and POC in $_{constant}$pH were rinsed with artificial seawater free of HEPES buffer and supersaturated with respect to calcite ($\Omega = \sim 4$) after filtration. Rinsing the culture medium off the GF/F filters was necessary because remains of organic buffer on the filter would have otherwise contributed ~ 40 μg of carbon to TPC and POC measurements. POC filters were stored for 2 h in a desiccator, containing fuming HCl solution, to remove all inorganic carbon. After 6 h of drying at 60°C, POC and TPC were measured using an isotope ratio mass spectrometer combined with an elemental analyzer (EuroEA, Hekatech GmbH). Particulate inorganic carbon (PIC) was calculated as the difference of TPC and POC. Four POC samples of $_{constant}$pH were lost during measurement.

Chl *a* filters were homogenized with glass beads for 5 min in 10 mL of 90% acetone and centrifuged for 10 min at 5500 rounds per minute and 0°C. The supernatant was measured fluorometrically (Welschmeyer 1994) using a Turner 10-AU fluorometer.

Cell numbers and cell volume were determined with a Coulter Counter Z series (Beckman Coulter) at the beginning and the end of the main experiment, ~ 4 h after the light period started. Cell numbers were determined only at the beginning and the end to avoid the buildup of a large headspace in the culture bottles. Cell diameters of *E. huxleyi* were calculated from cell volume estimates assuming a spherical cell shape (Paasche 2001). The Coulter Counter was calibrated prior to the experiments with polystyrene beads of certified diameter (10 μm). Growth rates (μ) were calculated from cell numbers according to:

$$\mu = \frac{\ln(t_{fin}) - \ln(t_0)}{d} \quad (3)$$

where t_0 and t_{fin} are the cell numbers at the beginning and the end of the experiment, respectively, and d is the duration of the experiment in days. Production rates of POC, PIC, and Chl *a* were calculated by multiplying growth rates with the cellular content of the respective parameter.

Statistical analyses and data fitting—The data were analyzed by a nonlinear regression model. Therefore, a high number of treatment levels was set up with no replication. This approach was chosen because it provides more quantitative information for ecological modeling compared to an analysis of variance, without loss of power (Cottingham et al. 2005). Coefficients of determination (R^2) and p-values of the applied regression model are given in the figure legends.

Growth, carbon, and Chl *a* production rates, which increased with increasing CO_2 concentrations and leveled off at saturating conditions, can be described by Michaelis–Menten kinetics in the form of:

$$V = \frac{V_{max} \times fCO_2}{K_m + fCO_2} \quad (4)$$

where V is growth or production rate at a certain fCO_2, V_{max} is the theoretical maximum of growth or production, and K_m is the fCO_2 at which the maximum is half-saturated. The Michaelis–Menten concept was used to fit the data of $_{constant}$pH. The Michaelis–Menten kinetic was modified by subtracting a linear term from Eq. 4 when growth and production did not remain at maximum values but started to decrease again towards higher fCO_2. The modified Michaelis–Menten equation reads as

$$V = \frac{X \times fCO_2}{Y + fCO_2} - s \times fCO_2 \quad (5)$$

where s is the sensitivity constant, and X and Y are random fit parameters. V_{max} and K_m can be calculated from a fit with Eq. 5 by the following procedure. Eq. 5 has to be differentiated with respect to fCO_2 and set equal to zero to find the maxima of Eq. 5:

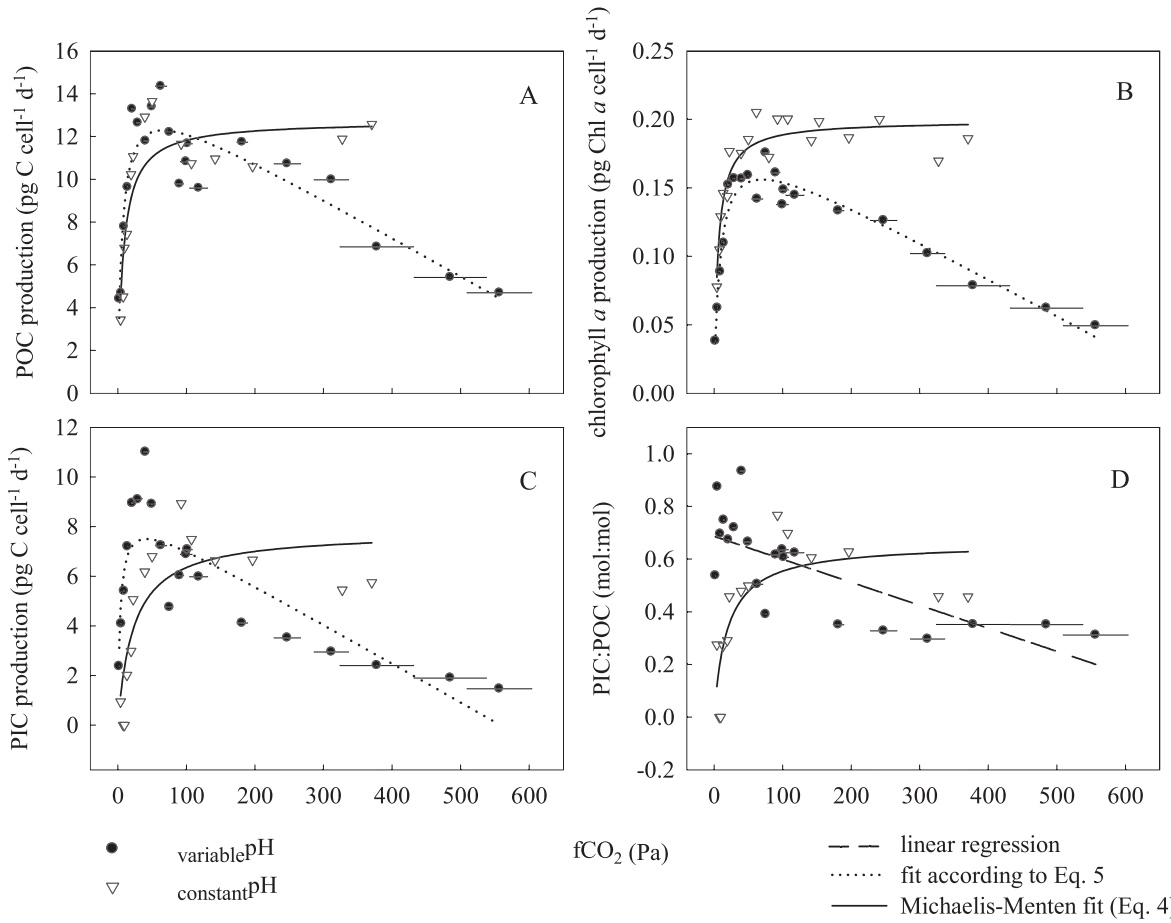

Fig. 4. Cellular POC, Chl *a*, and PIC production rates and PIC : POC ratios in $_{\text{variable}}$pH and $_{\text{constant}}$pH in relation to fCO_2. (A) POC production (dotted line $R^2 = 0.80$, $p < 0.0001$; solid line $R^2 = 0.77$, $p < 0.0001$), (B) Chl *a* production (dotted line $R^2 = 0.93$, $p < 0.0001$; solid line $R^2 = 0.87$, $p < 0.0001$), (C) PIC production (dotted line $R^2 = 0.70$, $p < 0.0001$; solid line $R^2 = 0.70$ $p = 0.0001$), (D) PIC : POC ratio (dashed line $R^2 = 0.54$, $p = 0.0001$; solid line $R^2 = 0.61$, $p = 0.0006$). Horizontal bars denote the change in fCO_2 over the course of the experiment. The biological response data are plotted against the means of the initial and final fCO_2 values.

$$\frac{\partial(V)}{\partial(\mathrm{fCO_2})} = 0 = \frac{X}{Y \times \mathrm{fCO_2}} - \frac{X \times \mathrm{fCO_2}}{(Y \times \mathrm{fCO_2})^2} - s \qquad (6)$$

Eq. 6 has to be solved for fCO2 to yield

$$\mathrm{fCO_2} = \sqrt{\frac{X \times Y}{s}} - Y \qquad (7)$$

The fCO_2 value calculated from Eq. 7 has to be inserted in Eq. 5. The resulting V equals the theoretical maximum—i.e., V_{max}. To calculate K_m from fits with Eq. 5, V_{max}, which has been calculated from Eq. 6 and 7 before, has to be divided by 2 (i.e., $V_{max}/2$) and substituted with V from Eq. 5. This equation has to be solved for fCO_2 and reads

$$\mathrm{fCO_2} = K_m = \left(\frac{1}{2} \times \frac{X - s \times Y - \frac{V_{max}}{2}}{s}\right) - \sqrt{\left(\frac{1}{2} \times \frac{X - s \times Y - \frac{V_{max}}{2}}{s}\right)^2 - \left(\frac{1}{2} \times \frac{V_{max} \times Y}{s}\right)} \qquad (8)$$

where the calculated fCO_2 value is the fCO_2 where the theoretical maximum from a fit with Eq. 5 is half-saturated (i.e., K_m).

Scanning electron microscopy (SEM)—Ten milliliters of sample were filtered by gravity on a polycarbonate filter (0.2-μm pore size). Five milliliters of a 20% ethanol solution (20% ethanol in 80% deionized water), was added to the sample at the point when only ~ 1 mL of the sample was left. This procedure was repeated with a 40%, 60%, 80%, 90%, 95%, and 100% ethanol solution and then with a 100% bis(trimethylsilyl)amine solution. Once the filter fell dry, it was immediately put in a petri dish and dried in a desiccator. The dried samples were kept in the desiccator until they were sputtered with gold-palladium and processed in the scanning electron microscope. This procedure conserves the organic parts of the cells which would otherwise tend to collapse during air-drying due to the high surface tension of the water inside the cells.

The degree of malformation of individual coccoliths was determined by assigning each coccolith to a certain category (Kaffes et al. 2010) with "incomplete," "normal," "slightly malformed," and "strongly malformed"

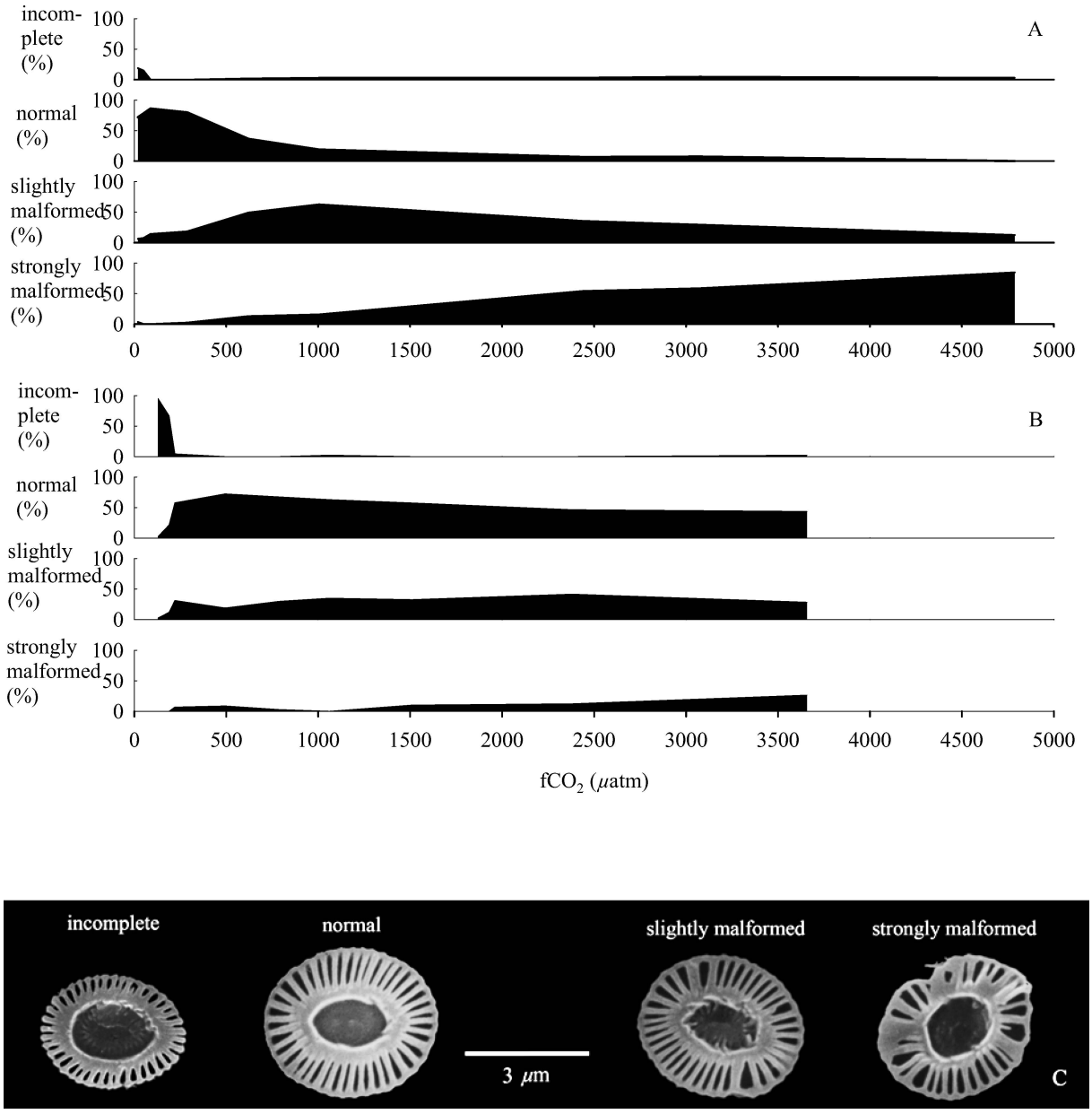

Fig. 5. Morphology of coccoliths in relation to fCO_2. (A) Samples from $_{variable}$pH. Samples were taken at fCO_2 levels of 2, 5, 9, 29, 63, 101, 247, 311, and 485 Pa. (B) Samples from $_{constant}$pH. Samples were taken at fCO_2 levels of 13, 19, 22, 50, 80, 108, 153, 241, and 371 Pa. (C) Distal view of coccoliths representative for classifications used in panels A and B.

(Fig. 5C). An average of ~ 50 coccoliths was analyzed for the treatments.

Results

Carbonate system—All carbonate system parameters, with the exception of $[CO_2]$, changed fundamentally differently with increasing fCO_2 in $_{variable}$pH compared to $_{constant}$pH. Most pronounced differences occurred in pH and $[CO_3^{2-}]$. With increasing fCO_2, pH remained constant in $_{constant}$pH whereas it was decreasing in $_{variable}$pH (Fig. 2C). $[CO_3^{2-}]$ decreased in $_{variable}$pH but increased in $_{constant}$pH (Fig. 2E). Because the saturation state of calcite ($\Omega_{calcite}$) is a function of $[CO_3^{2-}]$, it changed proportionally to $[CO_3^{2-}]$ (Fig. 2F). DIC and $[HCO_3^-]$ increased in both experiments, albeit differently (Fig. 2B,D).

DIC drawdown in the course of both experiments was estimated from total particulate carbon buildup. According to this, DIC drawdown was always well below 100 μmol kg^{-1} of the initial DIC concentration. The maximum change in pH in $_{constant}$pH was always below 0.02.

Growth rate, cell diameter, and organic matter production—Growth rate, mean cell diameter, POC, and Chl *a* production displayed distinct patterns in $_{constant}$pH and

Table 1. fCO_2 levels (Pa) in $_{variable}$pH and $_{constant}$pH at which maximum rates of individual processes are half-saturated (K_m). V_{max} represents the calculated maximum rate for each of the processes. *See* text for details about calculations of K_m and V_{max}.

	$_{variable}$pH	$_{constant}$pH
K_m		
Growth rate	2.7	1.7
Cell diameter	0.8	0.6
POC production	4.6	7.6
Chl *a* production	5.9	5.5
PIC production	2.7	22.8
V_{max}		
Growth rate (d^{-1})	1.1	1.1
Cell diameter (μm)	4.8	4.7
POC production (pg C $cell^{-1}$ d^{-1})	12.3	12.7
Chl *a* production (pg Chl *a* $cell^{-1}$ d^{-1})	0.16	0.2
PIC production (pg C $cell^{-1}$ d^{-1})	7.5	8

$_{variable}$pH. All four parameters increased similarly from low to intermediate fCO_2 where they reached their highest level. While they decreased linearly at $_{variable}$pH from intermediate to high fCO_2, all four parameters remained rather constant in $_{constant}$pH (Figs. 3, 4A,B). Because we observed three major regions where these measured physiological parameters show a characteristic response with fCO_2, we divide the whole fCO_2 range into three distinct ranges. The low fCO_2 range (0 to ~ 20 Pa) is characterized by a strong increase of growth and production rates in both experiments. The intermediate range (between ~ 20 and ~ 100 Pa) corresponds to the part of the response curve where growth and production rates have their particular optima, while the high fCO_2 range is defined as the part of the response curve above these optima.

Growth rate and cell diameter reached their highest measured values at ~ 20 Pa in both experiments. Both growth rate and mean cell diameter started to diverge considerably in $_{variable}$pH compared to $_{constant}$pH at ~ 100 Pa and 200 Pa, respectively (Fig. 3A,B). Highest measured POC production rates of about 14 pg $cell^{-1}$ d^{-1} in $_{variable}$pH and $_{constant}$pH were reached at approximately 80 Pa (Fig. 4A). Highest Chl *a* production rates were also reached at ~ 80 Pa in both experiments. In contrast to growth rate, mean cell diameter, and POC production, where highest absolute values were always similar in both experiments, highest Chl *a* production is consistently higher in $_{constant}$pH (0.2 pg $cell^{-1}$ d^{-1}) compared to $_{variable}$pH (~ 0.16 pg $cell^{-1}$ d^{-1}) (Fig. 4B). Note, however, that the light source of the fluorometer was exchanged in between measurements of the two data sets which might have led to these slight differences in absolute values.

Calcification—Calcification rates in $_{variable}$pH increased strongly from lowest to intermediate fCO_2 values of about 40 Pa and started to decrease above that value. The decrease from intermediate to higher fCO_2 is similar to previous studies (Riebesell et al. 2000; Zondervan et al. 2001) who used the same strain. PIC : POC showed a decreasing trend in $_{variable}$pH throughout the whole fCO_2 range. Calcification rates in $_{constant}$pH also increased from low to intermediate fCO_2 levels, but the increase is not as steep as in $_{variable}$pH (Fig. 4C; Table 1). Calcification rates and PIC : POC displayed a slight decrease in the high fCO_2 range in $_{constant}$pH (Fig. 4C,D). However, follow-up experiments with the same constant pH setup but different constant pH levels (pH_f 8.3 and 7.7; data not shown) showed calcification rates and PIC : POC remaining high up to fCO_2 levels which, in some treatments, were even higher than in the constant-pH experiment presented here. Hence, the slightly lower values in this study do not seem to indicate a real trend towards decreasing calcification and PIC : POC at high fCO_2 under constant pH.

SEM documented an increasing degree of malformation at fCO_2 levels above ~ 40 Pa in $_{variable}$pH (Figs. 5B, 6A–F). Coccoliths could not be found on the cell surface at the highest fCO_2 level (i.e., ~ 600 Pa). However, 2% out of 300 examined cells revealed visible signs of internal coccoliths which have not been egested to the cell surface (Fig. 6F), and we occasionally found free coccoliths on the SEM sample showing signs of dissolution. In contrast to $_{variable}$pH, malformations were on average less pronounced at high fCO_2 in $_{constant}$pH (Figs. 5C, 6G–L). Coccoliths started to be incomplete in the low fCO_2 range of $_{constant}$pH at ~ 19 Pa ($\Omega_{calcite} = 1$) (Figs. 5C, 6H) and were completely absent below ~ 12 Pa (none out of 300 cells had any visible signs of coccoliths below $\Omega_{calcite}$ of ~ 0.4) (Fig. 6G).

Discussion

In this study we extended the fCO_2 range toward lower and higher levels to investigate physiological responses in the ubiquitous coccolithophore *E. huxleyi*. To separate the effects of CO_2 and pH, pH was kept constant with increasing fCO_2 in a second experiment by using an organic buffer.

Growth rate, POC, and Chl a *production from low to intermediate fCO_2 (2–100 Pa)*—It has been the subject of discussion which carbonate system parameter is ultimately responsible for reduced growth and production rates at

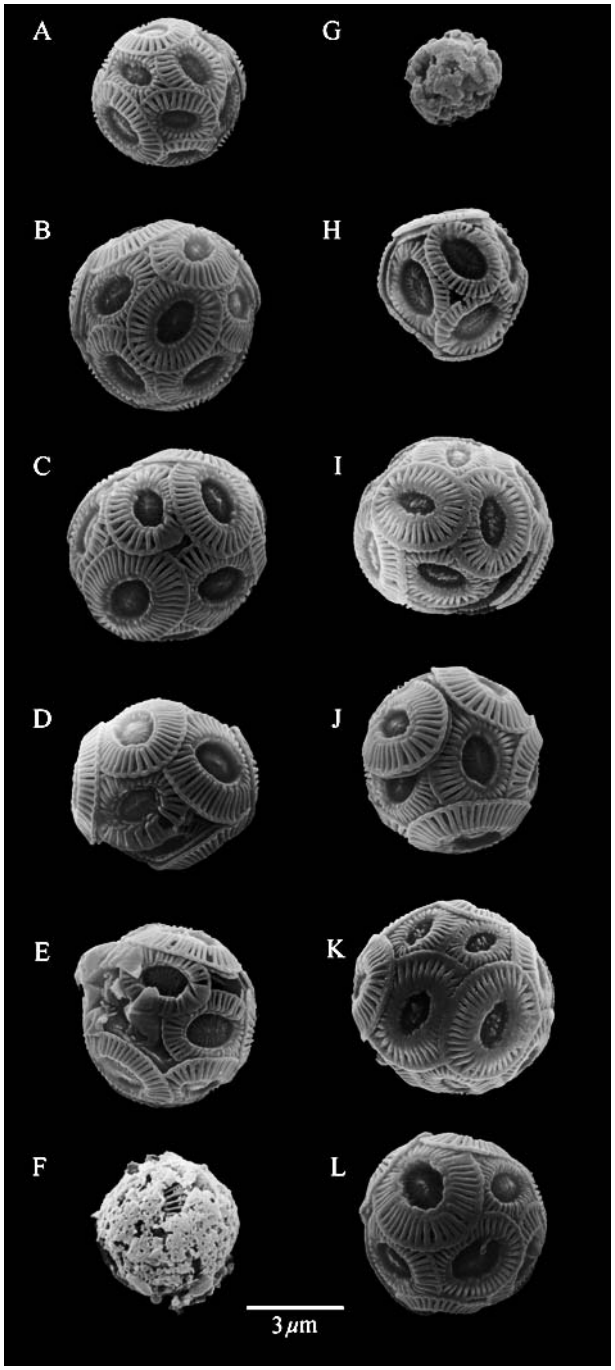

Fig. 6. SEM micrographs of *Emiliania huxleyi* at different carbonate chemistry conditions. The left column shows cells of the $_{variable}$pH experiment (A, B, C, D, E, F) while the right column shows cells of the $_{constant}$pH experiment (G, H, I, J, K, L). (A) fCO_2 = 2 Pa, pH_f = 9.06, $\Omega_{calcite}$ = 14.7; (B) fCO_2 = 29 Pa, pH_f = 8.24, $\Omega_{calcite}$ = 5.0; (C) fCO_2 = 63 Pa, pH_f = 7.96, $\Omega_{calcite}$ = 2.9; (D) fCO_2 = 102 Pa, pH_f = 7.78, $\Omega_{calcite}$ = 2; (E) fCO_2 = 312 Pa, pH_f = 7.32, $\Omega_{calcite}$ = 0.74; (F) fCO_2 = 557 Pa, pH_f = 7.08, $\Omega_{calcite}$ = 0.4; (G) fCO_2 = 4 Pa, pH_f = 7.98, $\Omega_{calcite}$ = 0.2; (H) fCO_2 = 13 Pa, pH_f = 8.00, $\Omega_{calcite}$ = 0.7; (I) fCO_2 = 50 Pa, pH_f = 7.99, $\Omega_{calcite}$ = 2.6; (J) fCO_2 = 108 Pa, pH_f = 8.00, $\Omega_{calcite}$ = 6; (K) fCO_2 = 241 Pa, pH_f = 8.00, $\Omega_{calcite}$ = 13.3; (L) fCO_2 = 371 Pa, pH_f = 8.01, $\Omega_{calcite}$ = 21.

low-CO_2, high-pH conditions in marine phytoplankton (Riebesell et al. 1993; Chen and Durbin 1994). As pointed out by Goldman (1999), it is virtually impossible to draw conclusions about the key carbonate chemistry parameter for growth and production in experiments where CO_2 and pH covary. In experiments where CO_2 and pH did not covary, it has been proposed that high pH is the limiting factor for growth rates at low-CO_2, high-pH conditions (Hansen et al. 2007). In contrast to this interpretation, we suggest that low CO_2 rather than high pH is responsible for reduced growth and organic carbon production rates in the low fCO_2 range of both experiments due to the following reasons. Despite the pronounced differences in the carbonate chemistry conditions between $_{variable}$pH and $_{constant}$pH (Fig. 2), growth, POC, and Chl *a* production rates increase in a similar way in both experiments from low to intermediate fCO_2 (Figs. 3, 4A,B; Table 1). Because no such similarity can be found in relation to any other carbonate system parameter, the consistency of the trends in relation to CO_2 supports the notion that the concentration of CO_2 is the responsible parameter at sub-saturating conditions. This, however, does not mean that CO_2 is the only carbon source utilized by *E. huxleyi*. It has been shown earlier that HCO_3^- is an additional inorganic carbon source for *E. huxleyi* (Paasche 1964; Rost et al. 2003; Schulz et al. 2007). The reason why external [CO_2] may still be the key parameter limiting growth, POC, and Chl *a* production rates at low fCO_2 can be explained by considering inorganic carbon fluxes between the cells and the seawater. *E. huxleyi* actively increases its intracellular CO_2 concentration to levels higher than those of the surrounding medium (Rost et al. 2003; Schulz et al. 2007) to increase the efficiency of the carbon-fixing enzyme ribulose-1,5-bisphosphate-carboxylase/oxygenase. If the CO_2 concentration is higher inside the cytosol than in the surrounding medium and the concentrated CO_2 is not instantly fixed into organic compounds, then part of the actively accumulated inorganic carbon will leak out of the cells because cell membranes are to some extent permeable to CO_2. High leakage of CO_2 out of the cells can lead to an increased energy demand for inorganic carbon uptake to compensate for leakage, or to reduced CO_2 fixation if the cell does not fully compensate for CO_2 loss via the carbon concentrating mechanisms (Falkowski and Raven 2007). Leakage of CO_2 increases if the CO_2 gradient between the cytosol and the external medium increases (Sharkey and Berry 1985). In our experiments, this CO_2 gradient was probably larger at low external fCO_2 so that the loss of CO_2 via leakage and therefore the reduction in carbon fixation rates could have been more pronounced at these conditions. Indeed, it has been observed for several other species that leakage of CO_2 strongly increased at fCO_2 levels below $\sim$ 20 Pa (Rost et al. 2006; Trimborn et al. 2008), which coincides with the CO_2 level below which a strong decrease in growth rates and POC production rates was found in the study presented here (Figs. 3A, 4A).

In this context, it is interesting to have a closer look at data by Hansen et al. (2007), who proposed high pH rather than low CO_2 to be responsible for reduced growth at low-CO_2, high-pH conditions. Plotting their measured growth

rates in relation to fCO_2 shows that growth rates nicely correlate with fCO_2 regardless whether the pH is normal (8.1) or comparatively high (up to 9.2). Hence, decreasing growth rates at low-CO_2, high-pH conditions as observed by Hansen et al. (2007) can actually also be interpreted to depend on external CO_2 concentration and therefore do not necessarily have to be a consequence of high pH.

Growth rate, POC, and Chl a *production from intermediate to high fCO_2 levels (100–600 Pa)*—Growth rates, POC, and Chl *a* production started to decrease in the high fCO_2 range at $_{variable}$pH range whereas they remained rather constant at $_{constant}$pH (Figs. 3, 4A,B). These fundamental differences cannot be related to different HCO_3^- or CO_2 concentrations because [HCO_3^-] and [CO_2] increased in both experiments at high fCO_2 (Fig. 2A,D). Carbonate system parameters that could potentially explain the different trends are pH or [CO_3^{2-}] since only these two parameters have opposing trends with increasing fCO_2 in $_{variable}$pH compared to $_{constant}$pH (Fig. 2C,E). Considering the large availability of CO_2 and HCO_3^- in the high fCO_2 range, it seems unlikely that differences in [CO_3^{2-}] were responsible for the observed differences between constant and variable pH incubations. Therefore, the difference in pH most likely explains the observed differences between $_{variable}$pH and $_{constant}$pH in the high fCO_2 range. Indeed, high [H^+] in seawater seems to correspond with high [H^+] inside phytoplankton cells (Coleman and Colman 1981; Nimer et al. 1994; Suffrian et al. 2011), which was shown to lead to decreased growth rates in *E. huxleyi* (Nimer et al. 1994). The negative effect of high intracellular [H^+] may result from an increased [H^+] in the stroma of the chloroplast, which could lead to a reduced CO_2 fixation efficiency (Werdan et al. 1975; Coleman and Colman 1981).

Calcification—Previous studies examining the effect of ocean acidification on *E. huxleyi* found decreasing calcification rates for CO_2 concentrations and pH levels projected for the year 2100 compared to present-day conditions (Riebesell et al. 2000; Sciandra et al. 2003; Delille et al. 2005). However, not all studies confirm the decreasing trend in calcification with increasing fCO_2 (Buitenhuis et al. 1999; Iglesias-Rodriguez et al. 2008; Langer et al. 2009). Contradictory results have been hypothesized to result from genotypic variations within different strains of *E. huxleyi* (Langer et al. 2009). If other strains also show optimized growth, primary production, and calcification rates at certain carbonate chemistry conditions, then observed strain-specific differences might reflect different strain-specific carbonate chemistry optima, potentially depending on the environmental conditions at the time and location at which the strain was originally isolated. Results presented in this study for the strain B92/11 are well in line with results presented in Riebesell et al. (2000), who used the same strain 10 yr earlier. In both studies, highest calcification rates were found at current atmospheric fCO_2 levels of about 40 Pa and declined from that point onwards. Based on these results, it can be concluded that during this 10-yr culturing period this strain did not change the general response of calcification to increased fCO_2 and decreased pH.

From low to intermediate fCO_2, the trends in calcification rates of $_{variable}$pH compared to $_{constant}$pH were neither similar in relation to fCO_2 (Fig. 4C) nor to any other carbonate system parameter (data not shown). According to this, there is no clear evidence for the key carbonate chemistry parameter(s) responsible for calcification rates at sub-saturating conditions. Currently, most studies favor HCO_3^- as the substrate for calcification while others favor CO_2 and HCO_3^- (*see* review by Paasche 2001).

In the fCO_2 range above ~ 40 Pa, calcification rate decreased in $_{variable}$pH whereas it remained at higher levels in $_{constant}$pH. We suggest that this difference is mainly caused by differences in seawater pH. The formation of calcium carbonate intracellularly leads to a production of H^+. H^+ has to be removed or neutralized to avoid a drop of the intracellular pH. The removal of H^+ is relatively easy at high seawater pH since the electrochemical gradient between in- and outside the cell is comparatively large (Mackinder et al. 2010). At decreasing seawater pH, the electrochemical gradient between the cell and the seawater might become smaller and H^+ removal from the cytosol therefore more difficult (Taylor et al. 2011; Suffrian et al. 2011).

The degree of malformation in coccoliths has been proposed to be a direct consequence of the seawater carbonate chemistry at high-CO_2, low-pH conditions. (Riebesell et al. 2000; Langer et al. 2006; Müller et al. 2010). SEM micrographs presented in our study confirm this for the high fCO_2 range in $_{variable}$pH. However, an increased frequency of malformed coccoliths could neither be found at very low fCO_2, high-pH conditions in $_{variable}$pH nor could it be found with the same frequency over the whole fCO_2 range in $_{constant}$pH (Figs. 5, 6). This suggests that malformations of coccoliths are mainly induced by seawater pH_f below ~ 8.

In the highest fCO_2 treatment of $_{variable}$pH, we did not find coccoliths on the cell surface using SEM. As most cells on the microscope slide were slightly damaged and the cell interior exposed, we examined those cells for the presence of internal coccoliths. In six out of 300 cells examined by SEM we found intact coccoliths inside the cells that had not yet been egested to the cell surface (Fig. 6F). In addition, we occasionally found free coccoliths showing clear signs of dissolution. These findings indicate that at least some cells were able to produce coccoliths at $\Omega_{calcite}$ values below 0.4 but that these coccoliths rapidly dissolved after being egested to the cell surface and in contact with the corrosive seawater. This interpretation is supported by the inorganic carbon production rate of ~ 1.7 pg $cell^{-1}$ d^{-1} found at these conditions, suggesting that calcification was still ongoing (Fig. 4C). The second interpretation that coccoliths rapidly dissolved once they were egested is consistent with observations by Beaufort et al. (2007), who found clear signs of rapid coccolith dissolution to start when $\Omega_{calcite}$ becomes smaller than 0.4.

Similar to the 0.4-$\Omega_{calcite}$ treatment of $_{variable}$pH, we could not find any coccoliths on the cell surface in $_{constant}$pH in those treatments where $\Omega_{calcite}$ was 0.4 or lower. Because we found no signs of coccoliths inside 300 examined cells and not a single free coccolith on the SEM slides either, it remains unclear whether coccoliths in the low-$\Omega_{calcite}$

treatments of $_{constant}$pH are absent due to post-formation dissolution or if the cells did not produce coccoliths under these conditions. A major difference between the two experiments is that DIC is high at $_{variable}$pH when $\Omega_{calcite}$ becomes smaller than 0.4 while DIC is low at $_{constant}$pH when $\Omega_{calcite}$ becomes smaller than 0.4 (Fig 2F). The low availability of DIC might explain the absence of coccoliths in the low-$\Omega_{calcite}$ treatments of $_{constant}$pH. Possibly, the production of coccoliths was switched off at low DIC since calcification was competing with the more essential process of carbon fixation for limiting inorganic carbon and it could be too energy demanding to keep both processes operating.

Implications for future research—Our findings that key metabolic processes show optimum curves in response to carbonate chemistry changes, culminating at different levels of fCO_2, and that CO_2 and pH appear to be the key parameters responsible for the observed changes in metabolic rates at low and high fCO_2 levels, respectively, in this strain of *E. huxleyi* may help to develop more realistic parameterizations for coccolithophore calcification in response to future ocean acidification. According to these results, future research dealing with DIC uptake mechanisms of phytoplankton at sub-saturating conditions should have a closer look at the loss of CO_2 out of the cell, next to the uptake of CO_2 and HCO_3^- into the cells, because the loss of CO_2 at low external fCO_2 might, at least for some species, be a key process determining phytoplankton sensitivity to low CO_2. In the high fCO_2 range, further research should focus on the possible direct influence of pH. The results of this study may help to reconcile some of the contradictory observations on coccolithophore CO_2 and pH sensitivity, and contributes to improving our understanding of the cellular mechanisms involved in primary production and calcification.

Acknowledgments

We thank Andrea Ludwig and Kerstin Nachtigall for their support on particulate carbon measurements, Ute Schuldt and Sebastian Meier for their support during scanning electron microscopy, Sarah Febiri for taking care of the *Emiliania huxleyi* stock cultures, and the two anonymous reviewers for their valuable comments and suggestions on the manuscript. This research was funded by the Federal Ministry of Education and Research (Bundesministerium für Bildung und Forschung; 03F0608A) in the framework of the Biological Impacts of Ocean Acidification (BIOACID) project (subproject 3.1.1).

References

Beaufort, L., I. Probert, and N. Buchet. 2007. Effects of acidification and primary production on coccolith weight: Implications for carbonate transfer from the surface to the deep ocean. Geochem. Geophys. Geosyst. **8:** Q08011, doi:10.1029/2006GC001493

Buitenhuis, E. T., H. J. W. De Baar, and M. J. W. Veldhuis. 1999. Photosynthesis and calcification by *Emiliania huxleyi* (Prymnesiophyceae) as a function of inorganic carbon species. J. Phycol. **35:** 949–959, doi:10.1046/j.1529-8817.1999.3550949.x

Caldeira, K., and M. E. Wickett. 2005. Ocean model predictions of chemistry changes from carbon dioxide emissions to the atmosphere and ocean. J. Geophys. Res. (C Oceans) **110:** C09S04, doi:10.1029/2004JC002671

Chen, C. Y., and E. G. Durbin. 1994. Effects of pH on the growth and carbon uptake of marine phytoplankton. Mar. Ecol. Progr. Ser. **109:** 83–94, doi:10.3354/meps109083

Coleman, J. R., and B. Colman. 1981. Inorganic carbon accumulation and photosynthesis in blue-green-alga as a function of external pH. Plant Physiol. **67:** 917–921, doi:10.1104/pp.67.5.917

Cottingham, K. L., J. T. Lennon, and B. L. Brown. 2005. Knowing when to draw the line: Designing more informative ecological experiments. Front. Ecol. **3:** 145–152, doi:10.1890/1540-9295(2005)003[0145:KWTDTL]2.0.CO;2

Danbara, A., and Y. Shiraiwa. 1999. The requirement of selenium for the growth of marine coccolithophorids, *Emiliania huxleyi*, *Gephyrocapsa oceanica* and *Helladosphaera* sp. (Prymnesiophyceae). Plant Cell Physiol. **40:** 762–766.

Delille, B., J. Harlay, I. Zondervan, S. Jacquet, L. Chou, R. Wollast, R. G. J. Bellerby, M. Frankignoulle, A. V. Borges, U. Riebesell, and J.-P. Gattuso. 2005. Response of primary production and calcification to changes of pCO_2 during experimental blooms of the coccolithophorid *Emiliania huxleyi*. Global Biogeochem. Cycles **19:** GB2023, doi:10.1029/2004GB002318

Dickson, A. G., J. D. Afghan, and G. C. Anderson. 2003. Reference materials for oceanic CO_2 analysis: A method for the certification of total alkalinity. Mar. Chem. **80:** 185–197, doi:10.1016/S0304-4203(02)00133-0

———, C. L. Sabine, and J. R. Christian. 2007. Determination of the pH of sea water using a glass/reference electrode cell, SOP 6a, p. 1–7. *In* A. G. Dickson, C. L. Sabine, and J. R. Christian [eds.], Guide to best practices for ocean CO_2 measurements. PICES Special Publication.

Falkowski, P. G., and J. A. Raven. 2007. Aquatic photosynthesis, 2nd ed. Princeton Univ. Press.

Gattuso, J. P., K. Gao, K. Lee, B. Rost, and K. G. Schulz. 2010. Approaches and tools to manipulate the carbonate chemistry, p. 41–52. *In* U. Riebesell, V. Fabry, L. Hansson, and J. P. Gattuso [eds.], Guide for best practices for ocean acidification research and data reporting. Publications Office of the European Union.

Goldman, J. C. 1999. Inorganic carbon availability and the growth of large marine diatoms. Mar. Ecol. Progr. Ser. **180:** 81–91, doi:10.3354/meps180081

Guillard, R. R., and J. H. Ryther. 1962. Studies of marine planktonic diatoms. I. *Cyclotella nana* Hustedt, and *Detonula confervacea* (cleve) Gran. Can. J. Microbiol. **8:** 229–239, doi:10.1139/m62-029

Hansen, H. P., and F. Koroleff. 1999. Determination of nutrients, p. 159–228. *In* K. Grasshoff, K. Kremling, and M. Ehrhardt [eds.], Methods of seawater analysis. Wiley-VCH.

Hansen, P. J., N. Lundholm, and B. Rost. 2007. Growth limitation in marine red-tide dinoflagellates: Effects of pH versus inorganic carbon availability. Mar. Ecol. Progr. Ser. **334:** 63–71, doi:10.3354/meps334063

Iglesias-Rodriguez, M. D., P. R. Halloran, R. E. M. Rickaby, I. R. Hall, E. Colmenero-Hidalgo, J. R. Gittins, D. R. H. Green, T. Tyrrell, S. J. Gibbs, P. von Dassow, E. Rehm, E. V. Armbrust, and K. P. Boessenkool. 2008. Phytoplankton calcification in a high-CO_2 world. Science **320:** 336–340, doi:10.1126/science.1154122

IPCC. 2001. Climate change 2001: The scientific basis. Intergovernmental Panel on Climate Change.

Kaffes, A., S. Thoms, S. Trimborn, B. Rost, G. Langer, K. U. Richter, A. Köhler, A. Norici, and M. Giordano. 2010. Carbon and nitrogen fluxes in the marine coccolithophore *Emiliania huxleyi* grown under different nitrate concentrations. J. Exp. Mar. Biol. Ecol. **393:** 1–8, doi:10.1016/j.jembe.2010.06.004

Kester, D., I. W. Duedall, D. N. Connors, and R. M. Pytkowicz. 1967. Preparation of artificial seawater. Limnol. Oceanogr. **1:** 176–179, doi:10.4319/lo.1967.12.1.0176

Langer, G., M. Geisen, K. H. Baumann, J. Kläs, U. Riebesell, S. Thoms, and J. R. Young. 2006. Species-specific responses of calcifying algae to changing seawater carbonate chemistry. Geochem., Geophys., Geosyst. **7:** Q09006, doi:10.1029/2005GC001227

———, G. Nehrke, I. Probert, J. Ly, and P. Ziveri. 2009. Strain-specific responses of *Emiliania huxleyi* to changing seawater carbonate chemistry. Biogeosciences **6:** 2637–2646, doi:10.5194/bg-6-2637-2009

LaRoche, J., B. Rost, and A. Engel. 2010. Bioassay, batch culture and chemostat experimentation, p. 81–94. *In* U. Riebesell, V. Fabry, L. Hansson, and J. P. Gattuso [eds.], Guide for best practices for ocean acidification research and data reporting. Publications Office of the European Union.

Lewis, E., and D. W. R. Wallace. 1998. Program developed for CO_2 system calculations [Internet]. ORNL/CDIAC-105. Oak Ridge (Tennessee): Carbon Dioxide Information Analysis Center, U.S. Department of Energy; 1997 October [accessed 2009 May 29]. Available from http://cdiac.ornl.gov/ftp/co2sys

Mackinder, L., G. Wheeler, D. Schroeder, U. Riebesell, and C. Brownlee. 2010. Molecular mechanisms underlying calcification in coccolithophores. Geomicrobiol. J. **27:** 585–595, doi:10.1080/01490451003703014

Müller, M. N., K. G. Schulz, and U. Riebesell. 2010. Effects of long-term high CO_2 exposure on two species of coccolithophores. Biogeosciences **7:** 1109–1116, doi:10.5194/bg-7-1109-2010

Nimer, N. A., C. Brownlee, and M. J. Merrett. 1994. Carbon dioxide availability, intracellular pH and growth rate of the coccolithophore *Emiliania huxleyi*. Mar. Ecol. Progr. Ser. **109:** 257–262, doi:10.3354/meps109257

Paasche, E. 1964. A tracer study of the inorganic carbon uptake during coccolith formation and photosynthesis in the coccolithophorid *Coccolithus huxleyi*. Physiol. Plant. **3:** 1–82.

———. 2001. A review of the coccolithophorid *Emiliania huxleyi* (Prymnesiophyceae), with particular reference to growth, coccolith formation, and calcification–photosynthesis interactions. Phycologia **40:** 503–529, doi:10.2216/i0031-8884-40-6-503.1

Riebesell, U., D. A. Wolf-Gladrow, and V. Smetacek. 1993. Carbon dioxide limitation of marine phytoplankton growth rates. Nature **361:** 249–251, doi:10.1038/361249a0

———, and P. D. Tortell. In press. Effects of ocean acidification on pelagic organisms and ecosystems. *In* J.-P. Gattuso and L. Hansson [eds.], Ocean acidification. Oxford Univ. Press.

———, I. Zondervan, B. Rost, P. D. Tortell, R. E. Zeebe, and F. M. M. Morel. 2000. Reduced calcification of marine plankton in response to increased atmospheric CO_2. Nature **407:** 364–367, doi:10.1038/35030078

Rost, B., K. U. Richter, U. Riebesell, and P. J. Hansen. 2006. Inorganic carbon acquisition in red tide dinoflagellates. Plant Cell Environ. **29:** 810–822, doi:10.1111/j.1365-3040.2005.01450.x

———, U. Riebesell, S. Burkhardt, and D. Sultemeyer. 2003. Carbon acquisition of bloom-forming marine phytoplankton. Limnol. Oceanogr. **48:** 55–67, doi:10.4319/lo.2003.48.1.0055

Roy, R. N., L. N. Roy, K. M. Vogel, C. Porter-Moore, T. Pearson, C. E. Good, F. J. Millero, and D. C. Campbell. 1993. Thermodynamics of the dissociation of boric acid in seawater at S = 35 from 0 degrees C to 55 degrees C. Mar. Chem. **44:** 243–248.

Sabine, C. L., R. A. Feely, N. Gruber, R. M. Key, K. Lee, J. L. Bullister, R. Wanninkhof, C. S. Wong, D. W. R. Wallace, B. Tilbrook, F. J. Millero, T. H. Peng, A. Kozyr, T. Ono, and A. Rios. 2004. The oceanic sink for anthropogenic CO_2. Science **305:** 367–371, doi:10.1126/science.1097403

Schulz, K. G., B. Rost, S. Burkhardt, U. Riebesell, S. Thoms, and D. A. Wolf-Gladrow. 2007. The effect of iron availability on the regulation of inorganic carbon acquisition in the coccolithophore *Emiliania huxleyi* and the significance of cellular compartmentation for stable carbon isotope fractionation. Geochim. Cosmochim. Acta **71:** 5301–5312, doi:10.1016/j.gca.2007.09.012

Sciandra, A., J. Harlay, D. Lefèvre, R. Lemée, P. Rimmelin, M. Denis, and J. P. Gattuso. 2003. Response of coccolithophorid *Emiliania huxleyi* to elevated partial pressure of CO_2 under nitrogen limitation. Mar. Ecol. Progr. Ser. **261:** 111–122, doi:10.3354/meps261111

Sharkey, T. D., and J. A. Berry. 1985. Carbon isotope fractionation of algae as influenced by an inducible CO_2 concentrating mechanism, p. 389–401. *In* W. J. Lucas and J. A. Berry [eds.], Inorganic carbon isotope uptake by aquatic photosynthetic organisms. American Society of Plant Physiologists.

Stoll, M. H. C., K. Bakker, G. H. Nobbe, and R. R. Haese. 2001. Continuous-flow analysis of dissolved inorganic carbon content in seawater. Anal. Chem. **73:** 4111–4116, doi:10.1021/ac010303r

Suffrian, K., K. G. Schulz, M. Gutowska, U. Riebesell, and M. Bleich. 2011. Cellular pH measurements in *Emiliania huxleyi* reveal pronounced membrane proton permeability. New Phytol. **190:** 595–608, doi:10.1111/j.1469-8137.2010.03633.x

Taylor, A. R., A. Chrachri, G. Wheeler, H. Goddard, and C. Brownlee. 2011. A voltage-gated H^+ channel underlying pH homeostasis in calcifying coccolithophores. PLoS Biol. **9:** e1001085, doi:10.1371/journal.pbio.1001085

Trimborn, S., N. Lundholm, S. Thoms, K. U. Richter, B. Krock, P. J. Hansen, and B. Rost. 2008. Inorganic carbon acquisition in potentially toxic and non-toxic diatoms: The effect of pH-induced changes in seawater carbonate chemistry. Physiol. Plant. **133:** 92–105, doi:10.1111/j.1399-3054.2007.01038.x

Welschmeyer, N. A. 1994. Fluorometric analysis of chlorophyll *a* in the presence of chlorophyll *b* and phaeopigments. Limnol. Oceanogr. **39:** 1985–1992, doi:10.4319/lo.1994.39.8.1985

Werdan, K., H. W. Heldt, and M. Milovancev. 1975. Role of pH in regulation of carbon fixation in the chloroplast stroma—studies on CO_2 fixation in light and dark. Biochim. Biophys. Acta **396:** 276–292, doi:10.1016/0005-2728(75)90041-9

Wolf-Gladrow, D. A., U. Riebesell, S. Burkhardt, and J. Bijma. 1999. Direct effects of CO_2 concentration on growth and isotopic composition of marine plankton. Tellus (B Chem. Phys. Meteorol.) **51:** 461–476, doi:10.1034/j.1600-0889.1999.00023.x

Zondervan, I., R. E. Zeebe, B. Rost, and U. Riebesell. 2001. Decreasing marine biogenic calcification: A negative feedback on rising atmospheric pCO_2. Global Biogeochem. Cycles **15:** 507–516, doi:10.1029/2000GB001321

Associate editor: John Albert Raven

Received: 27 January 2011
Accepted: 27 July 2011
Amended: 01 August 2011